Metazoans, migrations, and the ocean's biological carbon pump

Jérôme Pinti[1], Tim DeVries[2,3], Tommy Norin[1], Camila Serra-Pompei[1], Roland Proud[4], David A. Siegel[2,3], Thomas Kiørboe[1], Colleen M. Petrik [5], Ken H. Andersen [1], Andrew S. Brierley[4], André W. Visser[1]

[1]VKR Centre for Ocean Life, Technical University of Denmark, 2800 Kongens Lyngby, Denmark

[2] Department of Geography, University of California, Santa Barbara, California 93106, USA

[3] Earth Research Institute, University of California, Santa Barbara, California 93106, USA

[4] Pelagic Ecology Research Group, School of Biology, Gatty Marine Laboratory, Scottish Oceans Institute, University of St Andrews, St Andrews, Fife KY16 8LB, UK

[5] Department of Oceanography, Texas A&M University, 3146 TAMU, USA

Abstract

Diel vertical migration of fish and other metazoans actively transports organic carbon from the ocean surface to depth, contributing to the biological carbon pump. Here, we use a global vertical migration model to estimate global carbon fluxes and sequestration by fish and metazoans due to respiration, fecal pellets, and deadfalls. We estimate that fish and metazoans contribute 5.2 PgC/yr (2.1-8.8PgC/yr) to passive export out of the euphotic zone. Together with active transport, we estimate that fish are responsible for 20% (9-29%) of global carbon export, and 32% (18-43%) of oceanic carbon sequestration, with forage and deep-dwelling mesopelagic fish contributing the most. This essential ecosystem service could be at risk from unregulated fishing on the high seas.

Keywords— Diel Vertical Migrations, Food-webs, Game theory, Biological carbon pump, Carbon sequestration, Mesopelagic fish

Introduction

Many marine organisms – from zooplankton to fish – perform diel vertical migration (DVM) (*1–3*). The main explanation for DVM is a trade-off between feeding opportunity and predator avoidance. Organisms feed close to the surface during nighttime, and migrate to depth during daytime where risk from visual predators is reduced (*4*, *5*). Higher trophic levels have their own imperative to organise their vertical migration to take advantage of their migrating prey while avoiding predators. DVM within a marine pelagic community is therefore the product

of a co-adaptive game where many animals seek to optimize their migration patterns relative to the migration patterns of their respective prey, predators and con-specifics (*6–8*).

These interacting DVM patterns govern trophic interactions (*9*) and affect global biogeochemical cycles (*10*). Migrating organisms transport carbon obtained through feeding at the surface, to depth where it is released through respiration and excretion. This process, termed the active biological pump (or migrant pump), is highly efficient and facilitates the escape of organic material from remineralization close to the surface, unlike passive sinking during which particles get degraded by bacteria as they sink (*11*). The biological pump is one of the ocean's key ecosystem services, as it mediates the draw-down of atmospheric carbon dioxide by transporting surface carbon to the deep (*12*), where it can be sequestered for time scales ranging from decades to centuries (*13*). It has been estimated that in the absence of the biological carbon pump, atmospheric CO_2 concentrations may be up to 200 ppm higher (*14*).

Several studies have explored the effects of DVM on carbon export (*15–17*), but have mainly focused on exports mediated by zooplankton (*15*, *17–20*). Recent biogeochemical models estimate that active carbon fluxes mediated by migrating organisms range between 1 and 30 $\mathrm{mgCm^{-2}day^{-1}}$, corresponding to 14-18 % of the local passive sinking flux (*15*, *16*). However, these studies did not assess the carbon sequestration potential (amount of dissolved inorganic carbon held in the oceans when processes are at equilibrium) of these processes. Carbon sequestration is an important measure to report in addition to carbon export (rate of carbon being brought down below the euphotic zone, either actively or by passive sinking), as it does not only give an estimate of the strength of the biological pump but also of its efficiency (*10*).

The global contribution of fish to the active biological pump is currently poorly resolved (*21*, *22*). In particular, the contribution of mesopelagic fish is potentially of great importance, in part because of their high biomass, which has recently been estimated to be significantly higher than that of epipelagic fish (*23*, *24*). With biomass estimates ranging from 1.8 to 16 gigatonnes, mesopelagic fish harbour a huge potential for active carbon sequestration through their DVMs that span several hundred meters (*3*, *21*).

Here, we use a pelagic food-web model to investigate the global carbon export and sequestration potential due to different functional groups, including meso-zooplankton –zooplankton ranging from 0.2 to 2mm–, macro-zooplankton –from 2 to 20mm–, forage fish (planktivorous fish ranging from 4 to 30cm), mesopelagic fish, top predators, and jellyfish. We start by computing the optimal DVM patterns of all components of the food-web simultaneously, taking into account the feedbacks that individual behaviours can have on each other, as well as the consequences of light levels, temperature and oxygen concentration on the vital rates of these organisms (see Supplementary Material). We use spatially resolved realistic estimates of global biomasses to compute the equilibrium DVM patterns of the different populations, and use these global patterns to compute active carbon export mediated by each group, from both respiration at depth and sinking of their fecal pellets and carcasses. Finally, we combine our results with an ocean circulation inverse model (OCIM) (*25*, *26*) to estimate the total amount of carbon that is presently sequestered in the global ocean, and the sequestration timescale of respired carbon. See Supplementary Material for details of all calculations.

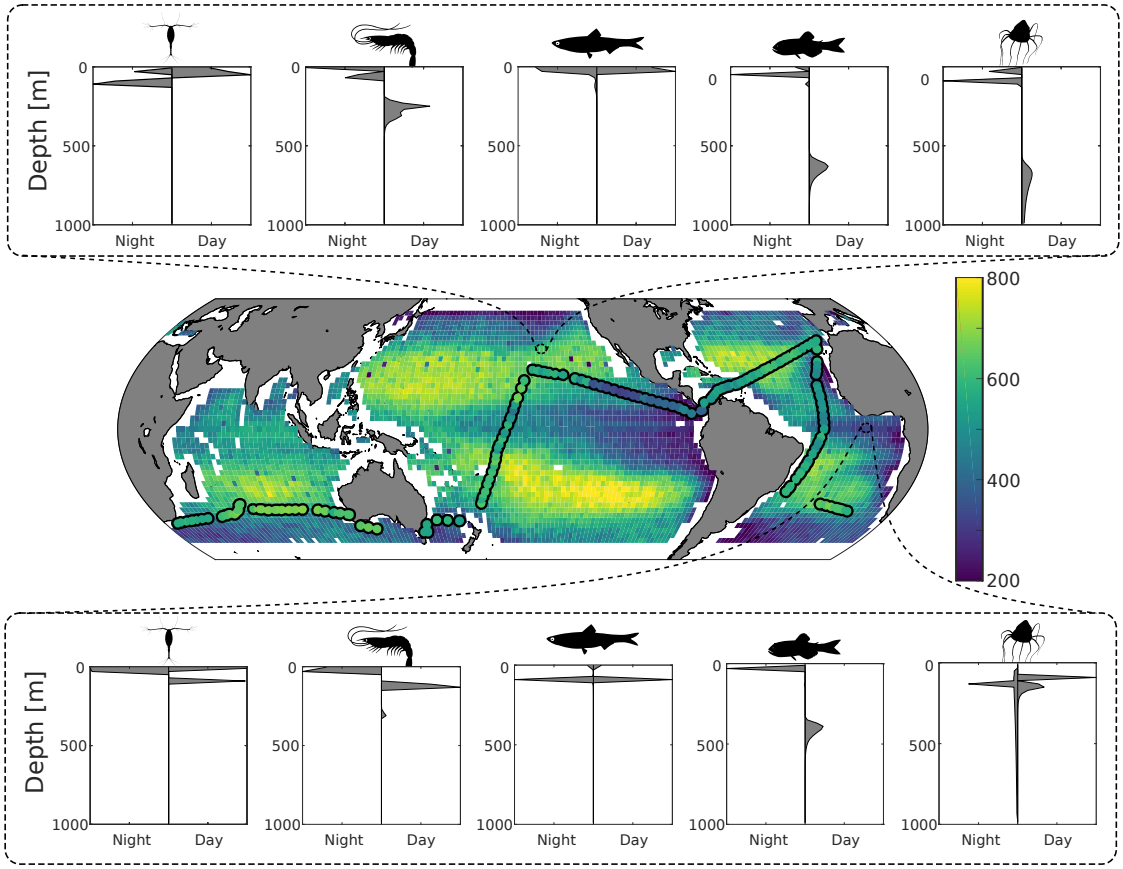

Figure 1: Top & bottom panels: predicted day and night depth distribution of mesozooplankton, macrozooplankton, forage fish, mesopelagic fish and jellyfish at 26°N 152°W and 7°S 0°E respectively. Large pelagic fish are not shown because they are assumed to be scattered throughout the water column at all times. Middle panel: Predicted fish mean depth during daytime, weighted by biomass. Circles overlaid are the observed mean depths weighted by echo intensity recorded using an echosounder operating at 38 kHz during the 2010 Malaspina expedition (*3*).

Results

We initialize the model with physiological parameters describing interactions between individuals and metabolic rates of the different functional groups, as well as the geographic distribution of physical parameters (light, temperature and oxygen levels) and the carbon biomass of different functional groups (see Supplementary Material). We base our estimates on a reference simulation with the most probable parameter values, and provide a range of uncertainties for all reported fluxes, carbon sequestered estimates, and sequestration timescales, by varying the most uncertain parameters of the model by a fixed fraction of the reference value (typically by 50% for biomasses, bacterial degradation rates and detritus sinking speeds – ranges are reported between brackets after the reference figures).

The predicted DVM patterns of the different functional groups generally match echosounder observations: meso-zooplankton and forage fish remain close to the surface, whereas macro-zooplankton and mesopelagic fish (as well as jellyfish) perform vertical migrations everywhere, sometimes with multimodal vertical distributions during part of the day (Figure 1). The biomass-weighted mean depth, taken as the model-predicted mean daytime depth of all fish weighted by biomass, is deeper in oceanic gyres (between 500-700 m deep), and shallower along the

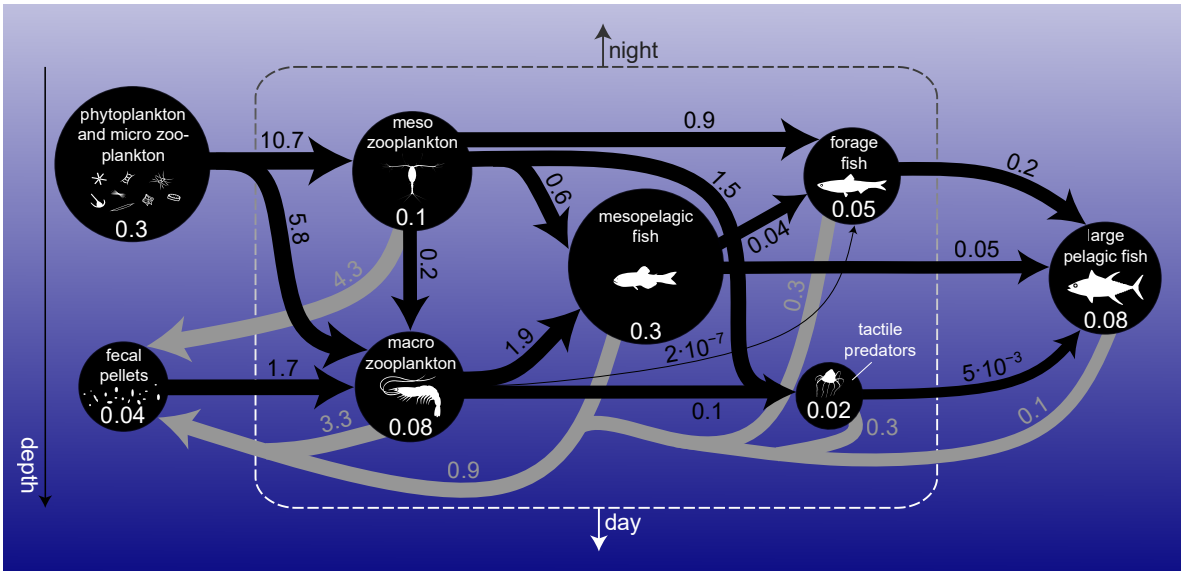

Figure 2: Food-web of the model. Biomass (circles) and fluxes (arrows) are integrated values over the global ocean in PgC (white numbers) and PgC yr^{-1} (black and grey numbers), respectively. Black arrows represent ingestion while grey arrows represent fecal pellet excretion. Arrow widths and circle diameters are proportional to the logarithm of the fluxes and biomasses they represent. Respiration losses are not represented here. The dashed box surrounds the functional groups that can perform DVM in the model, i.e. that optimize their day and night vertical distribution.

ocean margins and at the Equator (between 200-400 m). Even though low frequency (e.g. 38 kHz) echosounder observations can be biased by resonance as small fish with swim bladders contribute disproportionately to the signal (*24*), they can be used as a proxy for estimating the mean depth of water-column communities. The mean depth weighted by 38 kHz echo intensity collected during the circum-global Malaspina expedition (*3*) using a hull-mounted echosounder closely matches our predictions of biomass-weighted mean depth, and our global mean (517 m) is very close to a previous observation-based estimate of 525 m (*27*).

The global vertical distribution of organisms enables us to compute the strengths of trophic couplings between different functional groups in the model (figure 2). We find the strongest coupling between mesopelagic fish (total biomass of 0.32 PgC) and macro-zooplankton, with mesopelagic fish ingesting 1.9 (0.5-3.4) PgC of macro-zooplankton annually. Tactile predators are strongly coupled to meso zooplankton, as they account for almost 50% of meso zooplankton predation mortality. Deadfalls and fecal pellets excreted by all groups contribute to a passive sinking flux of 5.2 (2.1-8.8) PgC yr^{-1} at the base of the euphotic zone (see figure 3 for local estimates). Additionally, 2.3 (1.0-3.8) PgC yr^{-1} of fecal pellets and 0.5 (0.2-0.7) PgC yr^{-1} of carcasses are produced below the euphotic zone by organisms, which also respire 3.2 PgC yr^{-1} (1.3 (0.6-1.9) PgC yr^{-1} through basal respiration and 1.9 (0.7-3.5) PgC yr^{-1} through other losses) below the euphotic zone globally (see figures S10 and S11 for local estimates). Table 1 provides a summary of the carbon export due to the different pathways – basal respiration, fecal pellets, carcasses and other losses – for all functional groups. Assuming that the system is at steady state, we can also estimate the contributions of the different functional groups to carbon sequestration, as well as the corresponding residence times (figure 3 and table 1). Zooplankton are the most important contributors to carbon sequestration (meso- and macro-zooplankton contribute to the sequestration of 400 (200-800) and 600 (300-1100)

PgC respectively), followed by mesopelagic fish (400 (100-700) PgC sequestered in total), jellyfish (200 (100-500) PgC), and forage fish (100 (40-200) PgC). Carbon sequestered via the fecal pellets pathway remains in the ocean on a longer time scale than carbon sequestered via respiration (160 (90-270) years vs. 40 (20-50) years for all functional groups, table 1). In addition, carbon sequestered via degradation of fast-sinking fish fecal pellets or carcasses is stored on much longer time scales (from 330 (210-480) years for mesopelagic fish fecal pellets up to 630 (590-640) years for large pelagic fish carcasses) than carbon sequestered via pathways of slower-sinking fecal pellets such as meso-zooplankton (210 (100-370) years). While zooplankton produce the largest carbon fluxes, DIC produced via fish respiration or degradation of detritus originating from fish is stored more efficiently in the ocean's interior – all because larger organisms tend to remain deeper and because they produce larger particles that sink faster and thus escape remineralization in the upper parts of the water columns.

On a regional level, the absolute magnitude of the fecal pellet flux below the euphotic zone varies significantly, from less than 10 to more than 120 mgC m^{-2} day^{-1} (figure 3). Subtropical gyres have the lowest export, followed by the tropics, upwelling areas, North Atlantic and North Pacific, with the highest rates of carbon export by fecal pellets. However, the relative contribution of the different functional groups to carbon sequestration appears quite constant across the different regions of the ocean (figure S9). Zooplankton dominate carbon sequestration via fecal pellets excretion (more than 50 % of the total), followed by mesopelagic and jellyfish (around 23 and 11% respectively). Mesopelagic fish dominate carbon sequestration via the respiration pathway (more than 60% of the total) due to their deep daytime residence depths (figure 1).

Only a few datasets are available for comparing model predictions with observations. First, simulated weighted mean depths match the scarce observations available (figure 1 and S7, (*3*)). Second, we compare the simulated sinking flux with sediment traps data (*28*). While there are large differences between data and observations for some locations (up to 20 mgC m^{-2} day^{-1}, see figure S7), there is no global or regional bias in these differences (figure S8) and the predicted fluxes are of the same order of magnitude as those observed. A key constraint on carbon sequestration is apparent oxygen utilization (AOU), since the total respired carbon sequestration cannot exceed the amount implied by AOU given the stoichiometric relationship between oxygen consumption and dissolved inorganic carbon (DIC) production during respiration. Our carbon sequestration values generally match well with those expected from World Ocean Atlas AOU estimates (*29*), with a global R^2 of 0.76 (figure S12). WOA AOU predicts a carbon sequestration of 1770 PgC on the global ocean and a recent study (*30*) estimated that the interior oceans stores 1300 (± 230) PgC (compared to our estimates of 1790 PgC), but our spatial coverage accounts for only 63 % of the global ocean (no coastal areas nor latitudes higher than ±45°), suggesting that we overestimate global carbon sequestration, particularly in the low-latitude thermocline (figure S13). It may therefore be reasonable to scale our reported carbon sequestration values downward by 35% to account for this discrepancy, which is well within the reported uncertainty (Table 1). This scaling should not affect the relative importance of the higher vs. lower trophic levels contribution to carbon export or sequestration.

While the large number of parameters and high computational cost of each simulation prohibit a complete sensitivity analysis, we tested model sensitivity to 5 poorly-constrained parameters: bacterial degradation rate, fecal pellet sinking speed, biomass of all functional groups, biomass of mesopelagic fish only, and assimilation efficiencies. These parameters are anticipated to be those to which carbon export and sequestration are most

sensitive. Overall, the DVM patterns observed are very robust (figure S14). Carbon exported and sequestered vary significantly within sensitivity scenarios, but are mostly of the same order as the ranges of the parameter variations (table S1-S13), supporting the robustness of our results. In addition, we ran a more detailed Monte-Carlo sensitivity analysis for 5 water columns in 5 different ecoregions (subtropical gyres, tropical area, North Pacific, North Atlantic and Southern Ocean). This analysis confirms that the behaviour of organisms and passive and active fluxes are fairly robust to small changes in parameters (figures S16-S20). Respiration due to other losses, and to a lesser degree the sinking flux below the euphotic zone, are more sensitive to small changes in parameters than are basal respiration and the production of detritus (fecal pellets or carcasses) below the euphotic zone. The sensitivity to changes in parameter values was similar within ocean ecoregions (figures S16-20).

Discussion

Our results demonstrate that fish play a much more important role in the global carbon cycle than previously assumed – a hypothesis suggested by local estimates (*21*, *31*, *32*). Our model is not built on DVM or carbon flux observations, but on fundamental mechanistic principles defining the interactions between individuals within different functional groups. These interactions lead to realistic vertical migration patterns and carbon fluxes that are coupled to a global ocean circulation model to assess global carbon sequestration. In our model, fish (including mesopelagic fish, forage fish, and large predators) account for 20% (9-29%) of total carbon export and 32% (18-43%) of total carbon sequestration. The outsize influence of fish on carbon sequestration (relative to export) is due to the deep migration depths of mesopelagic fish, and the production of large fast-sinking fecal pellets, both of which lead to long sequestration times for the resulting respired DIC. The results are, to our knowledge, the first global mechanistic estimates of DVM patterns for different functional groups, and the first global estimates of fish-mediated carbon export and sequestration. They are in line with a recent literature review of local studies that estimated that fish were responsible for around 16.1 % (± 13 %) of carbon flux out of the euphotic zone (*22*).

Current global estimates of particle export below the euphotic zone (not resolved for functional groups) range between 4 and 12 PgC yr^{-1} (*33*, *34*), with several estimates clustered around 9-10 PgC yr^{-1} (*35–37*). Our model estimates a sinking flux out of the euphotic zone of 5.2 PgC yr^{-1}, mostly of zooplankton fecal pellets, which is in line with carbon export estimated by satellite-driven food web models (*34*, *38*). However, our model does not include the direct sinking of detrital aggregates derived from unicellular organisms, estimated to account for an additional 1-2 PgC^{-1} of export (*34*, *38*). Further, our model does not include coastal areas (shallower than 500 m) nor latitudes higher than $\pm 45°$. Coastal areas were not included because our model is unsuited to shallow continental shelf regions, and high latitudes were not included because of their seasonality. Specifically, seasonality can lead to large annual variations in DVM behaviour (*39*) coupled to zooplankton dormancy (*40*) that can be of importance to carbon export (*41*). With the same spatial coverage as our model, the SIMPLE-TRIM carbon export model (that estimates a global export flux of ∼9 PgC yr^{-1}, *37*) predicts a total export flux out of the euphotic zone of ∼6 PgC yr^{-1}, in close agreement with our estimates.

In addition to the passive sinking of fecal pellets and carcasses, our model also predicts carbon export by

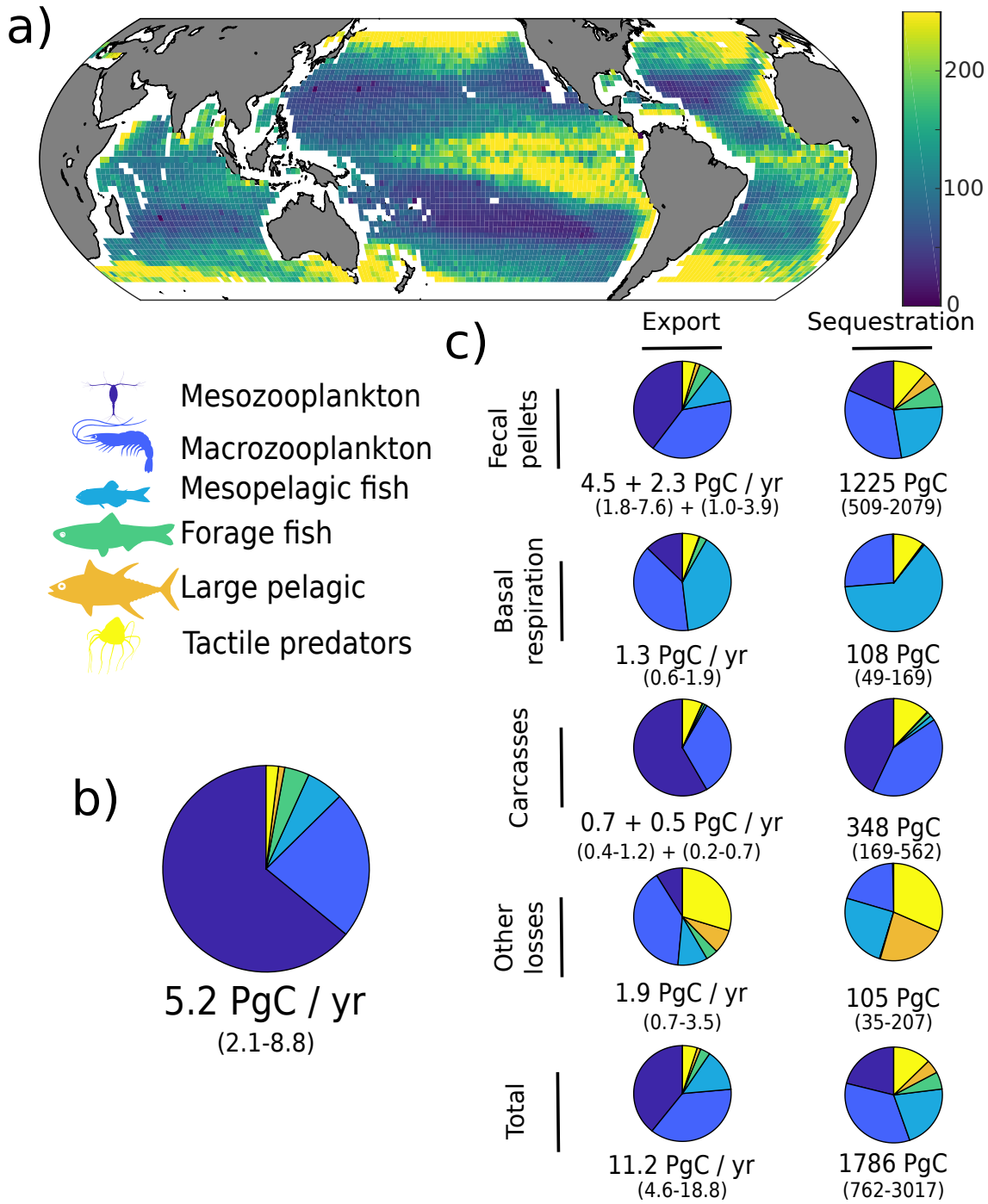

Figure 3: a) Predicted total export (active and passive) at the base of the euphotic zone (in mgC m^{-2} day^{-1}). b) Relative contribution of the different functional groups to the passive sinking flux at the base of the euphotic zone on a global scale. c) Relative contribution of the functional groups to export and sequestration (left and right column respectively) via the different pathways. For fecal pellets and carcass degradation, the first flux value corresponds to the passive sinking flux at the base of the euphotic zone, and the second to the active transport and production below the euphotic zone. For basal respiration and other losses, only the active transport and production below the euphotic zone are reported.

Table 1: Total export, corresponding sequestration, and sequestration time for the different pathways considered in the model. Respiration pathway corresponds to animal respiration, fecal pellets pathway to bacterial respiration due to fecal pellet degradation, carcasses to natural mortality and other losses to all other losses. The range provided is obtained with the different scenarios of the sensitivity analysis.

Organism	Respiration pathway			Fecal pellets pathway			Carcasses pathway			Other losses			Total		
	Export [PgC yr^{-1}]	Sequestr. [PgC]	Sequestr. time [yr]	Export [PgC yr^{-1}]	Sequestr. [PgC]	Sequestr. time [yr]	Export [PgC yr^{-1}]	Sequestr. [PgC]	Sequestr. time [yr]	Export [PgC yr^{-1}]	Sequestr. [PgC]	Sequestr. time [yr]	Export [PgC yr^{-1}]	Sequestr. [PgC]	Sequestr. time [yr]
Meso zoopl.	0.2	0.4	2	2.7	226	84	0.7	150	214	0.2	0.4	2	3.8	377	99
	(0.07 - 0.3)	(0.2-0.5)	(2-3)	(1.0 - 5.1)	(76-489)	(39-170)	(0.4 - 1.0)	(72-262)	(103-364)	(0.02 - 0.3)	(0.1-0.8)	(0.2-4)	(1.5 - 6.7)	(148-752)	(98-112)
Macro zoopl.	0.5	28	56	2.6	419	161	0.4	145	363	0.8	21	27	4.3	613	143
	(0.2 - 0.7)	(12-46)	(49-61)	(1.2 - 4.0)	(190-843)	(100-298)	(0.2 - 0.7)	(62-257)	(292-522)	(0.2 - 1.4)	(0-48)*	(0-35)*	(1.8 - 6.8)	(264-1194)	(143-175)
Meso-pelagic	0.5	68	136	0.8	287	359	9e-3	6	667	0.2	26	116	1.5	387	258
	(0.1 - 1.0)	(14-137)	(133-139)	(0.2 - 1.5)	(67-535)	(225-554)	(2e-3 - 0.02)	(1-11)	(508-716)	(0.07 - 0.3)	(8-41)	(104-134)	(0.4 - 2.8)	(90-724)	(225-259)
Forage fish	0.03	0.2	7	0.3	98	327	9e-3	5	579	0.08	0.3	3	0.4	104	260
	(0.01 - 0.04)	(0.06-0.3)	(3-7)	(0.1 - 0.4)	(42-162)	(196-511)	(5e-3 - 0.01)	(2-7)	(468-654)	(0.04 - 0.1)	(0.08-0.4)	(2-4)	(0.2 - 0.6)	(44-170)	(220-283)
Large pelagic	3e-3	0.4	143	0.1	57	570	2e-3	1	621	0.2	24	162	0.3	82	273
	(1e-3 - 5e-3)	(0.2-0.7)	(138-156)	(0.03 - 0.2)	(20-116)	(467-684)	(9e-4 - 3e-3)	(0.6-2)	(587-655)	(0.05 - 0.3)	(8-49)	(161-164)	(0.08 - 0.5)	(29-168)	(273-363)
Jellyfish	0.07	11	153	0.3	139	463	0.08	42	525	0.5	33	65	1.0	225	225
	(0.03 - 0.1)	(5-19)	(142-156)	(0.08 - 0.7)	(35-332)	(300-634)	(0.04 - 0.1)	(21-63)	(388-628)	(0.1 - 1.3)	(6-87)	(62-67)	(0.3 - 2.2)	(67-501)	(223-228)
Total	**1.3**	**108**	**86**	**6.8**	**1225**	**180**	**1.2**	**348**	**290**	**1.9**	**105**	**54**	**11.2**	**1786**	**159**
	(0.6 - 1.9)	**(49-179)**	**(61-100)**	**(2.8 - 11.5)**	**(509-2160)**	**(113-302)**	**(0.7 - 1.8)**	**(169-562)**	**(183-430)**	**(0.7 - 3.5)**	**(35-207)**	**(44-73)**	**(4.6 - 18.8)**	**(762-3017)**	**(159-161)**

*Here, the lowest sequestration value obtained for other losses was negative (and was truncated to 0), meaning that some parameter settings (very high mesopelagic fish biomass) are not compatible with a viable macro zooplankton population.

active diel vertical migration. Other modelling studies that have assessed the role of DVM on carbon export have relied on a few heuristics rather than mechanistic principles (*15*, *16*), and rarely considered functional groups separately to assess their relative importance (*15*). Their resulting estimates are lower than ours. Aumont et al. (*16*) estimated that all migrating organisms export about 1.0 PgC yr^{-1} below 150 m, and Archibald et al. (*15*) found that zooplankton organisms are responsible for the export of about 0.8 PgC yr^{-1} below the euphotic zone. Our model predicts a total active export below the euphotic zone of 6.0 PgC yr^{-1} due to vertical migrants and to predators of vertical migrants staying below the euphotic zone, of which half is due to macro-zooplankton. This large difference between our model and previous studies can be due to several factors. First, some studies considered the export below a 150 m deep reference, whereas we consider the export below the euphotic zone that is always shallower than 150 m (see figure S4). Further, comparison with observations suggest that they underestimated the biomass of functional groups such as mesopelagic fish (*16*). Local mesopelagic fish-mediated carbon export measurements estimate that between 15-17 % of the carbon flux is due to mesopelagic fish (*21*), a ratio in agreement with our results (14 % of the total flux due to mesopelagic fish).

Our results are relatively robust, as a factor 2 change in the most sensitive parameter values lead to a factor 2 change in exports. One of the most sensitive inputs is biomasses, and their global estimates are still uncertain. For example, mesopelagic fish global biomass estimates vary between 20 and 200 % of the reference estimate due to the uncertainty in translating echosounder observations into biomass estimates (*24*). Gelatinous zooplankton estimates are still highly imprecise (*42*), but potentially of considerable importance. A recent study (*43*) estimated that gelatinous zooplankton were responsible for a global export of 1.6-5.2 PgC yr^{-1} below 100 m. Even if this study encompasses coasts and high latitudes and has a fixed depth horizon, their estimate is still much higher than our estimate of a total export of 0.9 (0.3-2.2) PgC yr^{-1} below the euphotic zone for jellyfish, perhaps because their study –unlike this one– included gelatinous zooplankton that can also feed on phytoplankton and micro zooplankton.

We built our model by assuming general principles and all biological parameters were applied globally. Input variability (temperature, oxygen, biomasses) is the only factor that can lead to geographic differences in the food-web behaviour. The carbon budget is balanced in the model for each functional group, with the "other losses" acting as a buffer by encompassing all processes unaccounted for explicitly in the model. As a conservative estimate, we assume that these other losses are respired by organisms – a reasonable assumption when considering that carbon not currently considered in the bioenergetic budget would either be respired or used for reproduction.

Organisms and behaviours not included in our model may modify the estimated strength of the biological carbon pump, particularly at depth. Because of its daily temporal resolution, our model predicts that the entire mesopelagic community migrates to the surface at night. While this is counter to what happens in nature, as acoustic backscatter at depth is often detected at night by echosounders (*3*), the exact proportion of migrating organisms is unknown. In addition, as seafloor depth increases, another functional group of fish appears: bathypelagic fish. These fish constantly live below ∼1000 m, potentially migrating daily between bathyal depths (up 4000 m deep) and the mesopelagic zone, making up the lower bound of the Vinogradov ladder (*44*). These organisms, feeding on mesopelagic fish, would tend to increase the efficiency of the active biological carbon pump. The biomass of bathypelagic fish is, however, even more unreliably estimated than the biomass of mesopelagic

fish. Therefore, their potential contribution to global carbon export and sequestration is hard to assess. We can only postulate that carbon sequestrated because of bathypelagic fish migration would be sequestrated on very long time scales given the depths at which these organisms live.

As anthropogenic pressures increase, the last realm to remain somewhat undisturbed is the deep sea. This may change because of commercial incentives to fish on the vast resource that mesopelagic fish represents (*45*). It has been suggested that 50 % of the existing mesopelagic biomass can be sustainably extracted (*45*). However, this may have implications for carbon sequestration. If half the biomass of mesopelagic fish is extracted, then to first order that would reduce their contribution by 50 percent, i.e., 190 PgC (which is equivalent to 700 Pg CO_2). At € 25 per ton of CO_2 (CO_2 European Emission Allowances), the carbon off-set value of 50% of mesopelagic fish biomass would be € 17.2 billion. This demonstrates that mesopelagic ecosystems can have other advantages than harbouring a vast food resource.

Data, code and material

The source code (written in MATLAB) supporting this article has been uploaded as part of the supplementary material and is available at: `https://github.com/JeromeAqua/Global_contribution_fish`.

Acknowledgements

This work was supported by the Centre for Ocean Life, a VKR Centre of excellence funded by the Villum Foundation, and by the Gordon and Betty Moore Foundation (grant #5479). ASB and RP were funded in part through the EU BG3 project 'SUMMER' and BG8 project 'Mission Atlantic'.

Author contributions

JP designed the study with help from AWV and TK. RP, CMP, and ASB contributed biomass data. JP conducted the study with technical assistance from TDV, TN, CSP, DAS, TKA, KHA, and AWV. JP analysed results with help from TDV, DAS, CSP, TK, KHA, and AWV. JP wrote the manuscript with contributions from all authors. All authors approved the manuscript and agreed to be held personally accountable for their own contributions.

References

1. I. A. McLaren, *Journal of the Fisheries Research Board of Canada* **20**, 685–727, ISSN: 0015-296X (1963).

2. M. S. R. Onsrud, S. Kaartvedt, A. Røstad, T. A. Klevjer, *ICES Journal of Marine Science* **61**, 1278–1290, ISSN: 10543139 (2004).

3. T. A. Klevjer *et al.*, *Scientific Reports* **6**, 19873 (Apr. 2016).

4. T. M. Zaret, S. Suffern, *Limnology and Oceanography* **21**, 804–813, ISSN: 00243590 (1976).

5. W. Lampert, *Archiv her Hydrobiologie, Beiheft Ergebnisse der Limnologie* **39**, 79–88 (Dec. 1993).

6. D. M. Hugie, L. M. Dill, *Journal of Fish Biology* **45**, 151–169 (1994).

7. J. Pinti, A. W. Visser, *The American Naturalist* **193**, E65–E77, ISSN: 0003-0147 (Mar. 2019).

8. J. Pinti, T. Kiørboe, U. H. Thygesen, A. W. Visser, *Proceedings of the Royal Society B: Biological Sciences* **286**, 20191645 (Sept. 2019).

9. G. C. Hays, *Hydrobiologia* **503**, 163–170, ISSN: 00188158 (2003).

10. K. O. Buesseler, P. W. Boyd, *Limnology and Oceanography* **54**, 1210–1232, ISSN: 00243590 (2009).

11. P. W. Boyd, H. Claustre, M. Levy, D. A. Siegel, T. Weber, *Multi-faceted particle pumps drive carbon sequestration in the ocean*, 2019, DOI: `10.1038/s41586-019-1098-2`, (`http://dx.doi.org/10.1038/s41586-019-1098-2`).

12. P. G. Falkowski, R. T. Barber, V. Smetacek, *Science* **281**, 200–206, ISSN: 00368075 (1998).

13. T. DeVries, F. Primeau, C. Deutsch, *Geophysical Research Letters* **39**, 1–5, ISSN: 00948276 (2012).

14. E. Maier-Reimer, U. Mikolajewicz, A. Winguth, *Climate Dynamics* **12**, 711–722, ISSN: 14320894 (1996).

15. K. M. Archibald, D. A. Siegel, S. C. Doney, *Global Biogeochemical Cycles* **33**, 181–199 (2019).

16. O. Aumont, O. Maury, S. Lefort, L. Bopp, *Global Biogeochemical Cycles*, 1–22, ISSN: 08866236 (2018).

17. T. Gorgues, O. Aumont, L. Memery, *Geophysical Research Letters* **46**, 5387–5395, ISSN: 0094-8276 (2019).

18. A. Longhurst, A. Bedo, W. Harrison, E. Head, D. Sameoto, *Deep Sea Research Part A. Oceanographic Research Papers* **37**, 685–694, ISSN: 01980149 (Apr. 1990).

19. D. K. Steinberg *et al.*, *Deep Sea Research Part I* **47**, 137–158, ISSN: 09670637 (Jan. 2000).

20. A. N. Hansen, A. W. Visser, *Limnology and Oceanography* **61**, 701–710, ISSN: 19395590 (2016).

21. P. C. Davison, D. M. Checkley, J. A. Koslow, J. Barlow, *Progress in Oceanography* **116**, 14–30, ISSN: 00796611 (2013).

22. G. K. Saba *et al.*, *Limnology and Oceanography*, 1–26 (2021).

23. X. Irigoien *et al.*, *Nature communications* **5**, 3271, ISSN: 20411723 (Feb. 2014).

24. R. Proud, N. O. Handegard, R. J. Kloser, M. J. Cox, A. S. Brierley, *ICES Journal of Marine Science* **76**, ed. by D. Demer, 718–733, ISSN: 1054-3139 (May 2019).

25. T. DeVries, F. Primeau, *Journal of Physical Oceanography* **41**, 2381–2401, ISSN: 00223670 (2011).

26. T. DeVries, *Global Biogeochemical Cycles* **28**, 631–647, ISSN: 19449224 (2014).

27. R. Proud, M. J. Cox, A. S. Brierley, *Current Biology* **27**, 113–119, ISSN: 09609822 (2017).

28. M. J. Lutz, K. Caldeira, R. B. Dunbar, M. J. Behrenfeld, *Journal of Geophysical Research: Oceans* **112**, ISSN: 21699291, DOI: 10.1029/2006JC003706 (2007).

29. H. Garcia *et al.*, "WORLD OCEAN ATLAS 2018 Volume 3: Dissolved Oxygen, Apparent Oxygen Utilization, and Dissolved Oxygen Saturation", tech. rep. (Silver Spring, MD, 2019), p. 38, (https://www.nodc.noaa.gov/OC5/woa18/pubwoa18.html).

30. B. R. Carter *et al.*, *Global Biogeochemical Cycles* **35**, ISSN: 19449224, DOI: 10.1029/2020GB006623, (https://doi.org/10.1029/2020GB006623) (2021).

31. G. K. Saba, D. K. Steinberg, *Scientific Reports* **2**, 1–6, ISSN: 20452322 (2012).

32. J. M. Hudson, D. K. Steinberg, T. T. Sutton, J. E. Graves, R. J. Latour, *Deep-Sea Research Part I: Oceanographic Research Papers* **93**, 104–116, ISSN: 09670637 (2014).

33. S. A. Henson *et al.*, *Geophysical Research Letters* **38**, 10–14, ISSN: 00948276 (2011).

34. D. A. Siegel *et al.*, *Global Biogeochemical Cycles* **28**, 181–196, ISSN: 08866236 (Mar. 2014).

35. R. Schlitzer, *Deep-Sea Research Part II: Topical Studies in Oceanography* **49**, 1623–1644, ISSN: 09670645 (2002).

36. J. P. Dunne, R. A. Armstrong, A. Gnnadesikan, J. L. Sarmiento, *Global Biogeochemical Cycles* **19**, 1–16, ISSN: 08866236 (2005).

37. T. DeVries, T. Weber, *Global Biogeochemical Cycles* **31**, 535–555, ISSN: 19449224 (2017).

38. K. Bisson, D. A. Siegel, T. DeVries, *Frontiers in Marine Science* **7**, 1–15, ISSN: 22967745 (2020).

39. P. K. Prihartato, D. L. Aksnes, S. Kaartvedt, *Marine Ecology Progress Series* **521**, 189–200 (2015).

40. K. Bandara *et al.*, *Marine Ecology Progress Series* **555**, 49–64, ISSN: 01718630 (2016).

41. S. H. Jónasdóttir, A. W. Visser, K. Richardson, M. R. Heath, *Proceedings of the National Academy of Sciences* **112**, 12122–12126, ISSN: 0027-8424 (Sept. 2015).

42. C. H. Lucas *et al.*, *Global Ecology and Biogeography* **23**, 701–714, ISSN: 14668238 (2014).

43. J. Y. Luo *et al.*, *Global Biogeochemical Cycles* **34** (2020).

44. M. Vinogradov, *ICES reports*, 114–120 (1962).

45. M. A. St. John *et al.*, *Frontiers in Marine Science* **3**, 1–6, ISSN: 2296-7745 (2016).